Aust. J. Soil Res., 1976, **14**, 337–49

Infiltration and Water Movement in an *in Situ* Swelling Soil during Prolonged Ponding

T. Talsma[A] *and A. van der Lelij*[B]

[A] Division of Environmental Mechanics, CSIRO, P.O. Box 821, Canberra City, A.C.T. 2601.
[B] Water Resources Commission, Griffith, N.S.W. 2680.

Abstract

Infiltration, swelling, and water movement were studied during ponding on a swelling clay soil. The soil was uniform in texture and clay mineralogy to 2 m depth. Most structural heterogeneity, caused by gilgai and shrinkage cracks, had been removed by grading, cultivation, and pre-ponding irrigations. Measurements were made of infiltration, moisture content, soil water potential, hydraulic conductivity, bulk density, vertical soil swelling, and the effect of overburden on tensiometer readings.

Infiltration was rapid and water penetrated deeply during the first ponding day. Thereafter, qualitative agreement was found between measured infiltration and that expected from theory from 1 to 45 days after ponding. From 45 to 120 days after ponding, the development of a time-variable flow restriction near the soil surface prevented the attainment of a final, steady infiltration rate.

During ponding a transient water table developed, moisture profiles were distinctly hydric, and seepage to a deep water table or aquifer was not negligible. Core sample values of hydraulic conductivity agreed with those obtained from mean flux and potential gradients, although conductivity and infiltration rate varied greatly from place to place.

Measured swelling compared favourably with that calculated from bulk density changes. The maximum measured soil swelling, in the rather narrow range of moisture contents involved, was 25 mm. This is consistent with reported data on similar soils. Mean values of $\alpha = \Omega/P$ near saturation at 0·2 and 0·4 m depth were between 0·20 and 0·25, indicating that the effect of overburden potential on flow was not large.

Introduction

The theory of infiltration of ponded water into uniform, non-swelling soils is well established and has been adequately verified by laboratory and field studies; its description for swelling soils is, however, less advanced. Formal solutions (Philip 1969), although not worked out in detail, indicate that the effect of gravity should be less than in rigid soils. This has been demonstrated by Smiles (1974), who found in laboratory experiments on a swelling clay that infiltration could be described as an adsorption process for at least 7 days. The same predominance of capillary, over gravity, flow has been demonstrated in preliminary field experiments (Talsma 1976).

Many swelling soils are deeply cracked when dry, and this complicates the description of infiltration and soil water movement. While early work of Stirk (1954) suggested that significant crack formation and consequent high infiltration rates do not take place until the soil is relatively dry (pF $\simeq$ 4·5), subsequent studies (Allen and Braud 1966; Ritchie *et al.* 1972; Talsma 1976) show that the influence of cracks on water conduction persists at quite high moisture contents. Additionally, crack formation causes high variability of point infiltration rates, and the mean rate may strongly depend on infiltrometer or basin size (Allen and Braud 1966; Ritchie *et al.*

1972). The latter authors studied the effect of cracks on infiltration, but ignored vertical swelling.

We report here the results of a field study on a swelling soil. Experiments on infiltration, soil water movement, and aspects of soil swelling were conducted during the time (around 120 days) the field was ponded for rice growing. Pre-ponding irrigation for germination ensured that the soil profile was at an initial moisture content high enough that no visible cracks remained near the soil surface.

The Experimental Site

1. *Soil.* The experimental area was part of a 52 ha rice field near Coleambally, N.S.W. The soil is a vertisol; the dominant soil type is Wunnamurra clay (Wm), which, together with Tuppal clay loam (Tp), forms a gilgai complex (van Dijk and Talsma 1964). Before irrigation in 1963, the dry soil profile had wide cracks and surface elevation differences between the puff (Wm) and shelf (Tp) components of about 0·15 m. During 10 years' irrigation, however, surface elevation and surface texture differences have been largely erased by grading and cultivation.

Soil profile characteristics were obtained from eight bore logs at the site. Soil descriptions noted carbonate concretions to be present from the soil surface in five bores (Wm), while dark-coloured, soft topsoil intruded, through previous cracks, into the lighter coloured, denser subsoil to depths varying from 1·5 to 3 m. Former cracks and slickensides were observed at decreasing intensity with depth, in pits excavated to 1·5 m.

The soil profile was uniform in clay content (62%) to 2 m depth, and contained very little salt ($Cl^- < 4$ ppm). Although the main clay mineral group (percentage range 40–50 of <2 μm fraction) was identified as either montmorillonite or randomly interstratified, we note that the two groups exhibit very similar degrees of swelling.

2. *Plots.* Small plots were established approximately 20 m from the field boundary during the rice growing seasons of 1973–74 (plot 1) and 1974–75 (plot 2).

Plot 1 was about 4 × 8 m and accommodated three buffered ring infiltrometers, six swelling plates, two sets of tensiometers at 0·05, 0·1, 0·15, 0·3, 0·45, 0·6, and 0·9 m depth, and two sets of piezometers at 0·4, 0·7, 1, 1·3, and 1·65 m depth. Sufficient space was available nearby to obtain moisture samples, large cores for measurement of hydraulic conductivity, and samples for bulk density at various moisture contents, without unduly disturbing the plot.

Plot 2, about 5 × 20 m, was similarly instrumented, but had seven buffered infiltrometers. Duplicate tensiometers here were installed at 0·15, 0·3, 0·45, 0·6, 0·9, 1·2, and 1·5 m, and single tensiometers at 2 and 3 m depth. Duplicate piezometers were at 0·3, 0·6, 0·9, 1·2, and 1·5 m depth. Additional small areas near plot 2 were used late in the ponding period to study areal variability of infiltration rates and the effect of varying overburden load on tensiometer readings.

Experimental Details

1. Infiltration was measured frequently during initial ponding, and thereafter twice-weekly, by recording the water level in the inner ring with a depth gauge. Inner and outer rings, 0·9 and 1·5 m in diameter, were pushed 0·2 m into the soil. Details of the method are described by Talsma and van der Lelij (1976).

Areal variability of infiltration was studied with a single ring infiltrometer, pushed 0·05 m into the flooded soil. The ring was provided with an air-tight lid and connected, via a flexible tube, to a water supply in the form of a microburette floating horizontally on the ponded water surface. Provision was made for the escape of trapped air. Several spot measurements were made on two days.

2. Thin perforated steel plates (0·15 × 0·15 m) provided with a steel pin were used to measure vertical soil swelling. They were placed between thin sand layers on smooth, exposed surfaces at depths varying from 0·07 to 0·25 m below the preponded soil surface. The excavated soil was replaced after installation. Pin levels were measured by survey level with reference to a fixed bench mark anchored through a hollow pipe into the soil at 5 m depth.

3. Tensiometers at plot 1 were fitted with mercury manometers, those at plot 2 had individually calibrated vacuum gauges. Moisture potentials could be read more accurately with the former assembly, but their effective response time was greater than that of the gauge type. The main advantage of the gauges was their easier maintenance. On plot 1, tensiometers to 0·15 m depth were fitted with fritted glass disks (porosity 4, 1 cm diameter); at other depths, and on plot 2, 1 bar, ceramic tips 42 mm long and 18 mm diameter were used. The tensiometers were sealed into narrow, vertical access holes. Special care was taken to prevent leakage of ponded water along the tensiometer walls.

4. Piezometers consisted of 2·4 cm i.d. steel pipe; cavity lengths below the pipe were 10 cm. This design was a compromise for their dual purpose of assessing both positive water pressure and hydraulic conductivity at various depth intervals.

5. Additional hydraulic conductivity measurements were made between 0·2 and 0·3 m depth on large undisturbed cores (0·3 m diameter × 0·1 m long) enclosed in standard ring infiltrometers. These were taken after ponding and resaturated in the laboratory. Steady flow rates were maintained in a permeameter assembly which included provision to maintain an overburden load equal to the weight of the overlying wet soil and ponded water in the field. A sample of the 0–0·05 m topsoil, which slurries during ponding, was taken to the laboratory where it consolidated under its own weight in a 0·22-m long flow cell. A steady flow rate, using water containing mercuric chloride, was then maintained and hydraulic conductivity calculated, using measured potential gradients in the column.

6. Gravimetric moisture content was measured on soil samples obtained by a 0·12 m diameter auger. Duplicate samples were collected to 3 m depth on plot 1 and quadruplicate samples to 4·5 m on plot 2. These were taken before germination irrigations, and just before, and three times during, ponding. In the last case, samples were obtained by drilling rapidly within a 0·5 m long, 0·3 m diameter steel ring inserted deep enough into the ponded soil to prevent seepage into the hole. All holes were firmly backfilled. Samples, taken at 0·25 m depth intervals except near the surface (0·05 and 0·1 m intervals), were dried in an oven at 105°C.

7. Bulk density samples to 1·5 m depth were obtained with thin-walled (1·8 mm) core samplers, 8·6 cm i.d. and 5 cm long. These were lightly oiled and driven in with a single blow from a drop-hammer. Several samples were taken at various depths from pits near both plots, both before and after ponding. A limited number of deeper samples was obtained near plot 1 with a 'Proline' drilling rig.

8. Variation of overburden load was achieved by rapidly pumping water into an area enclosed by a 3 m diameter portable swimming pool which permitted a ponding depth variation of 0·53 m. Tensiometer response to change in overburden was measured on two sets of duplicate gauge-type tensiometers, inserted through plastic sleeves in the centre of the pool, to 0·2 and 0·4 m below the soil surface.

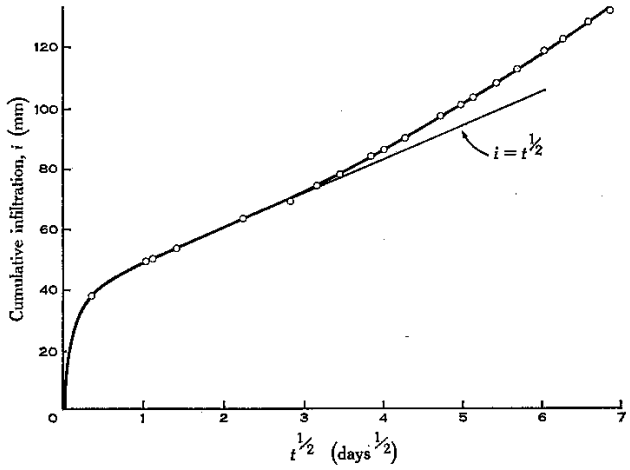

Fig. 1. Mean cumulative infiltration on plot 1 as a function of $t^{\frac{1}{2}}$.

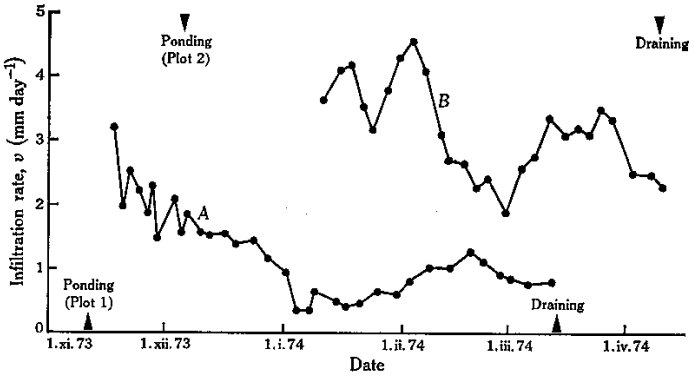

Fig. 2. Mean infiltration rates v. date on plot 1 (A) and plot 2 (B).

Results

Infiltration

The mean cumulative infiltration during the first seven weeks of ponding on plot 1 is shown in Fig. 1 as a function of $t^{\frac{1}{2}}$. We note that infiltration during the first day was quite rapid. Data points for days 2–8 fall essentially on a straight line, but linearity of $i(t^{\frac{1}{2}})$ is not maintained beyond day 9.

Mean infiltration rates (Fig. 2) over most of the ponding period fluctuated considerably. Nearly all infiltrometers showed distinct minima about 60 days after

ponding on both plots, with rates increasing after about 80 days and tending to decrease again by the end of ponding. Also, the large, buffered infiltrometers recorded widely different infiltration rates on any day, on both plots. This is seen in Fig. 3*a*, which shows the frequency distribution of arithmetic mean rates during days 50–125 after ponding. Fig. 3*b* shows the frequency distribution of infiltration rates obtained with the single ring infiltrometer. The two methods show distinct differences. Results from the large rings suggest a bimodal areal distribution of infiltration rate with a median value of $3 \cdot 7$ mm day^{-1}; those from the small ring show a positive skew distribution with a median value of $1 \cdot 6$ mm day^{-1}.

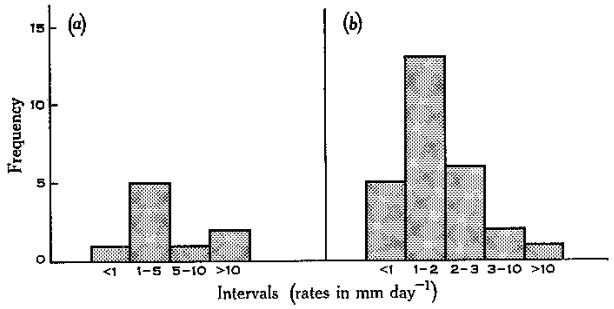

Fig. 3. Frequency distribution of infiltration rates (50–120 days after ponding): (*a*) large buffered infiltrometers; (*b*) small, single ring infiltrometer.

Potentials and Gradients

Figs 4*a* and 4*b* show, for plots 1 and 2, some selected average potentials, $\Psi + \Omega$, and calculated potential gradients, grad $\Phi = (\Psi + \Omega + z)/z$ (Ψ is unloaded moisture potential, Ω is overburden potential, and z is depth). Their magnitudes and trends during ponding are discussed in the next section, in relation to infiltration and water movement in the soil.

Moisture Profiles

Moisture content profiles are shown in Fig. 5, in the form of depth (z)/moisture ratio (ϑ) relationships. Gravimetric moisture contents (θ_g) may be deduced from these by the relationship $\vartheta = \theta_g \gamma_s$, values of the particle density, γ_s, being $2 \cdot 67$ at $0 \cdot 1$ m and about $2 \cdot 71$ for deeper layers. Numerals on the curves denote total volumetric moisture content of the sampled profile. Significant increases in moisture content occurred over the full sampling depth on plot 1 till mid-January (65 days after ponding); subsequent profiles in February (not shown in Fig. 5) and March were somewhat drier. The pre-irrigation profile on plot 2 was very wet due to considerable winter and spring rain following prolonged ponding for rice. Subsequent moisture uptake was slight. The wettest profile was again recorded in January (53 days after ponding). Driest and wettest profiles to 4 m depth on plot 2 are shown, on half scale, in the inset of Fig. 5.

Analysis of variance of the moisture content data showed that the soil profiles just before the end of ponding were significantly ($P = 0 \cdot 05$) drier than those obtained

about halfway (*c.* 60 days) through the ponding period. These differences were highly significant ($P = 0{\cdot}01$) for the deeper layers, from 1·8 to 3 m on plot 1, and from 2 to 4 m on plot 2.

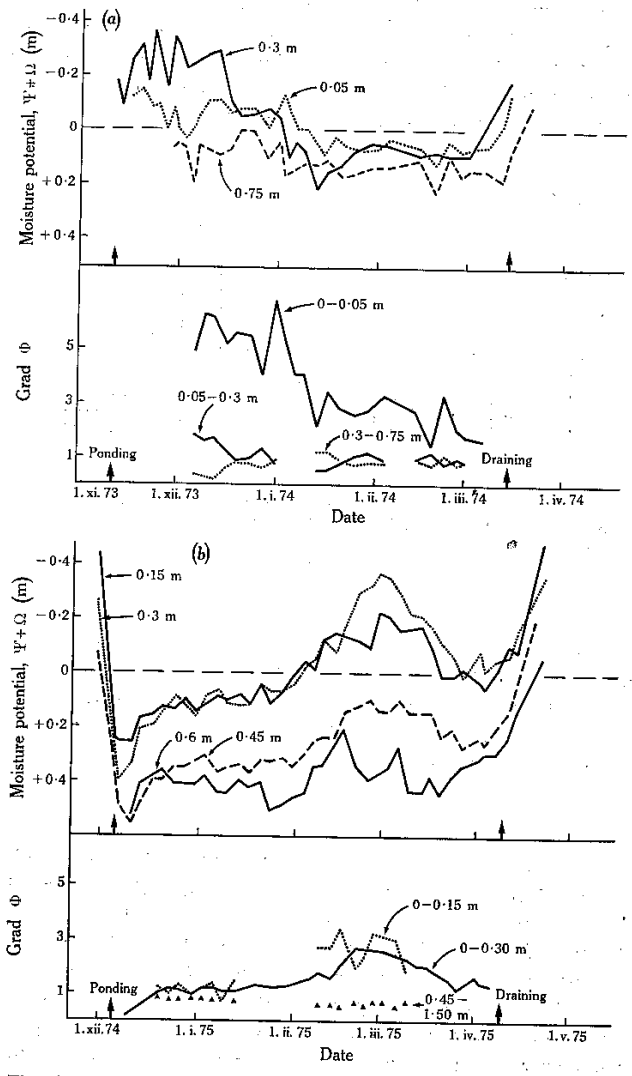

Fig. 4. Mean moisture potentials, $\Psi + \Omega$, and potential gradients, $(\Psi + \Omega + z)/z$, on (*a*) plot 1, and (*b*) plot 2.

Soil Density

On both plots bulk density, ρ_b, varied with moisture content, θ_g, to a depth of 0·8 m, where ρ_b was 1·41 over a range of θ_g from 0·28 to 0·32. Mean values of

ρ_b had, on the average, a standard deviation of 0·01 and a coefficient of variation around 3%. Results of all soil profile density measurements on plot 1 are summarized in Fig. 6, which shows values of void ratio, $e = (\gamma_s - \rho_b)/\rho_b$, for the driest and wettest soil profiles.

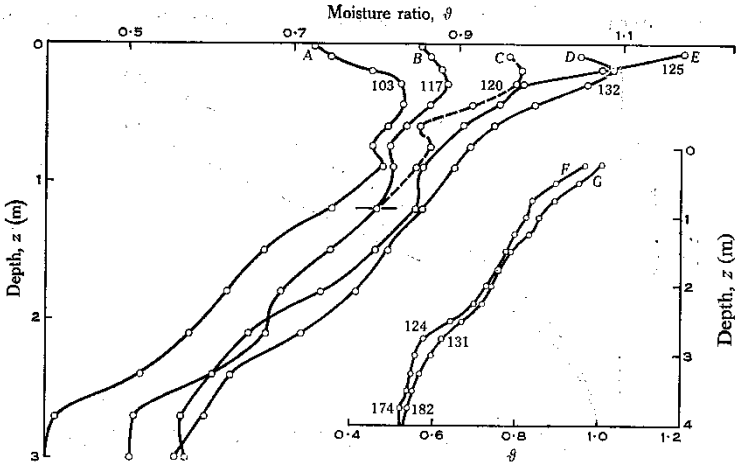

Fig. 5. Soil moisture content profiles; plots 1 and 2 (inset). *A*, 2 October 1973, before irrigation; *B*, 1 November 1973, after germination irrigation; *C*, 30 November 1973, 19 days after ponding; *D*, 14 January 1974, mid-season ponding; *E*, 14 March 1974, end of ponding; *F*, 9 September 1974, before irrigation; *G*, 17 January 1975, mid-season ponding. Numerals on curves denote total moisture contents in cm (on plot 2 to depths of 3 and 4 m).

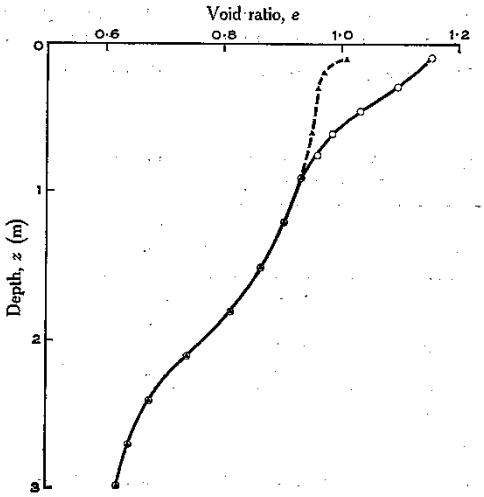

Fig. 6. Depth *v.* void ratio relationships on plot 1. ▲ - - - - - - ▲, 2 October 1973; ○ ——— ○, 14 January 1974.

Swelling

The extent of vertical soil swelling on plot 1 is shown in Fig. 7. Data points for the original 0·15 m soil depth represent the average rise of the swelling plates inserted

about this depth, taking as reference level their elevation just before the first germination irrigation. The change of elevation at the original 0·05 m depth has been calculated from this information and from bulk density changes between 0·05 and 0·15 m. Data for the original soil surface are not shown, since the corresponding surface is difficult to measure when ponded. Very little swelling (4 mm at 0·05 m depth) was recorded on plot 2, which was nearly saturated before irrigation.

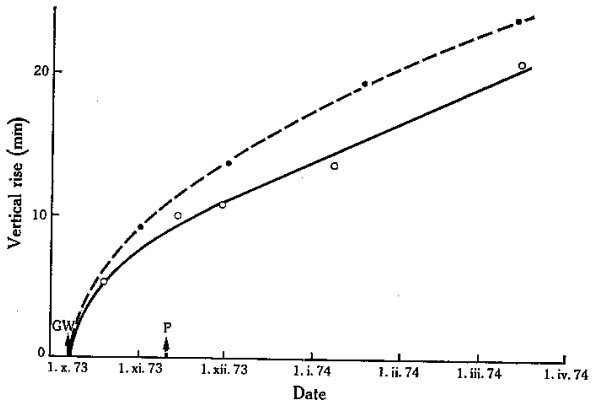

Fig. 7. Extent of vertical swelling of soil on plot 1. o ——— o, rise at 0·85 m depth; ● - - - - - - ●, rise at 0·05 m depth. GW, time of first germination irrigation; P, time of start of permanent ponding.

Directly measured swelling results should be consistent with those calculated from bulk density changes. Since Fig. 6 indicates no swelling beyond 0·8 m, the mean initial bulk density (1·38) of the 0·15–0·8 m layer should decrease to 1·34 as a result of soil profile swelling of 21 mm. This compares satisfactoriiy with a mean measured decrease to 1·33.

Table 1. Hydraulic conductivity, K, of slurried topsoil, laboratory experiment, flux $v = 3{\cdot}54$ mm day^{-1}

Depth interval (m)	ρ_b (g cm^{-3})	Grad Φ	K (mm day^{-1})
0·02–0·07	1·01	0·40	8·9
0·07–0·12	1·03	0·60	5·9
0·12–0·17	1·05	0·92	3·9
0·17–0·22	1·13	2·54	1·4

Hydraulic Conductivity

Values ($n = 16$) measured between 0·2 and 0·3 m depth ranged from 0·5 to 9·7 mm day^{-1}, with median and geometric mean values of 2·2 and 2·0 mm day^{-1}. Piezometer measurements of conductivity were even more variable and ranged from 0 to 37 mm day^{-1}. Highest values were found in the 0·4–1 m depth interval. Those between 1 and 2 m depth were around 1·5 mm day^{-1} with the exception of a single

value of 9 mm day^{-1} at 1·3 m depth. The results of the sterilized topsoil slurry experiment are given in Table 1.

Overburden

The effect of load variation on tensiometer readings is shown in Fig. 8. The potential increases during the period of increased loading. This is most clearly shown by tensiometer no. 15 at 0·4 m depth, but frequently (e.g. tensiometers nos 16 and 18 in Fig. 8) the effect appeared to be small, so that measured increases in potentials were close to the reading error of the gauge (0·07 m).

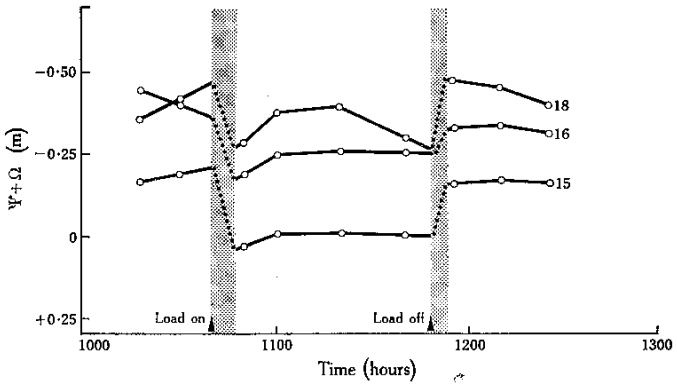

Fig. 8. Tensiometer response to load variation of 0·53 m of water, plot 2, 3 April 1975. Tensiometer numbers are marked on curves; 16 at depth 0·2 m, 15 and 18 at 0·4 m. Times taken to fully load and unload the soil are shaded.

Tensiometers *in situ* record values of $\Psi + \Omega$. Now $\Omega = \alpha P$ with

$$\alpha(\upsilon, P) = P^{-1} \int_0^P (\partial e/\partial \vartheta)_P \, dP, \qquad \vartheta = \vartheta$$

where the normal stress $P = P(0) + \int_0^z \gamma \, dz$,

Table 2. Mean values of $\alpha = \Omega/P$ and Ψ calculated from load variation of 0.53 m water

Depth (m)	$\Psi + \Omega$ $P(0) = 0{\cdot}13$ (m H_2O)	$\Psi + \Omega$ $P(0) = 0{\cdot}66$ (m H_2O)	α	$P(0)$ (m H_2O)	$\int_0^z \gamma \, dz$ (m H_2O)	Ψ (m H_2O)
0·2	−0·50	−0·37	0·24±0·11	0·13	0·34	−0·61
0·4	−0·27	−0·15	0·22±0·08	0·13	0·83	−0·48

$P(0)$ is vertical stress during surface loading, and γ is the apparent wet specific gravity (Philip 1971). We may then, to a good approximation, calculate α and Ψ from the expression for Ω and data such as given in Fig. 8, since only $P(0)$ was varied sub-

stantially during the experiment. Mean values of α, their standard deviation ($n = 5$), and of the unloaded moisture potential Ψ, so calculated, are given in Table 2.

Discussion

Infiltration

The early rapid infiltration of ponded water into relatively dry cracked soils is well documented (e.g. Allen and Braud 1966; Swartz 1966). It is not possible to interpret such behaviour in terms of swelling theory, which assumes complete soil homogeneity. We see here (Fig. 1) that, even in quite moist soil and in the absence of visible cracks, initial infiltration during ponding was still high.

Preponding, and initially ponded, water penetrated quickly to considerable depth, as shown directly by the moisture profiles in Fig. 5, but also by the sudden increase of potentials after ponding at all depths (Fig. 4*b*). These increases were much greater than could be accounted for by the effect of increased overburden (Table 2). The initial rapid movement of water throughout the profile is very likely to occur along preferential flow paths such as noted in the soil description. Water movement of this type has been documented by means of tracer dyes by Ritchie *et al.* (1972); we have not repeated such experiments. Subsequent infiltration was much slower and the soil on plot 1 gradually wetted up along its entire depth (Fig. 5) till mid-January (65 days after ponding).

Linear infiltration, i, $v.$ $t^{\frac{1}{2}}$ to 8 days after ponding suggests that sorption was dominant during this period, although this would occur from a highly irregular wetting 'front'. The average sorptivity, S, calculated from the linear portions of i $v.$ $t^{\frac{1}{2}}$ curves, such as shown in Fig. 1, was around 25 mm day$^{-\frac{1}{2}}$. This, together with a mean hydraulic conductivity, $K \simeq 2$ mm day^{-1} (see Results section) gives a time estimate, $t \leqslant 0{\cdot}02\,(S/K)^2$ for linear i $v.$ $t^{\frac{1}{2}}$ behaviour of the order of days rather than minutes as found for rigid soils (Talsma 1969).

Fig. 1 and other i $v.$ $t^{\frac{1}{2}}$ curves (not shown) indicate that infiltration after approximately one week proceeded as for rigid soils (Smiles and Colombera 1975) with both sorption and gravity contributing to flow, rather than being analogous to capillary rise in such soils (Philip 1971). This is to be expected, given the low values of α near saturation (Table 2). We note, however, that a long-time, steady rate was not achieved on either plot.

Water Movement

On plot 2 (Fig. 2) the low infiltration rates recorded from mid-February to early March (70–90 days after ponding) were associated with high flux gradients (Fig. 4*b*) near the surface. Although individual rates and gradients were quite variable, analysis of the primary data showed that both the increase in gradient and decrease of infiltration rate during this period differed significantly ($P = 0{\cdot}05$) from previous and subsequent recordings. At the same time the profile moisture content decreased slightly, but significantly (Fig. 5).

It follows that the hydraulic conductivity near the soil surface decreased temporarily. This has often been observed during prolonged flooding and is usually attributed to microbial activity (e.g. Allison 1947; Avnimelech and Nevo 1964). The hydraulic conductivity of the sterilized topsoil slurry (Table 1) remained quite high, so that the formation of a throttle by physical deterioration is unlikely.

The tensiometers on plot 1 (Fig. 4*a*) recorded, on the average, negative potentials near the surface for the first two months, in contrast to plot 2 (Fig. 4*b*) which, we recall, was close to saturation before ponding. The very low mid-season infiltration rates on plot 1 cannot therefore be clearly associated with a temporarily increased flux gradient near the surface. However, even after saturation the average gradient remained >1 between 0 and 0·05 m (Fig. 4*a*) and profile moisture content decreased (Fig. 5) for the remainder of the ponding period, again indicating flow restriction close to the soil surface.

Individual tensiometer records, rather than the average values, showed that flow was not throttled near the surface to the same extent everywhere. For instance, gradients between 0 and 0·05 m were generally <1 at one tensiometer location on plot 1 from mid-February to April, but $\gg 1$ at the other location. This is in agreement with infiltrometer results (Fig. 3), which indicated very variable surface intake rates.

During pre-ponding irrigations the subsoil wetted up rapidly (Fig. 5), so that tensiometers there may (and most did) record small negative, or even positive, potentials before or soon after ponding, while by-passed sections of the topsoil remained unsaturated for much longer. This often resulted in overall gradients <1 from 0·3 m to deeper layers soon after ponding (Fig. 4*a*).

Subsoil moisture potentials were predominantly positive during ponding. As a result a transient water table developed, and moisture profiles were distinctly hydric (Philip 1968). Comparison of mean infiltration and moisture storage in the soil (Fig. 5) shows that significant amounts of water infiltrated beyond the sampled profiles. This indicates that deep seepage under rice contributes to rising water tables in the irrigation areas.

Hydraulic Conductivity

Average flux gradients and infiltration rates may be used during periods of steady-state saturated flow to calculate hydraulic conductivity for comparison with other measured values. It is evident that both temporal (Fig. 2) and areal (Fig. 3) variation of the infiltration rate is such that this can only be done approximately here. The mean rate between 50 and 120 days after ponding (when steady state is approximated) was considerably less on plot 1 than on plot 2 (Fig. 2), and the large, buffered rings gave generally higher rates than the small, single rings (Fig. 3) during this period. Such data indicate the average infiltration rate for the whole field to be somewhere between 0·8 and 3·7 mm day^{-1}.

An independent estimate for the 52 ha field was possible for the 1974–75 season using the results of water balance studies (Talsma and van der Lelij 1976). This gave a final infiltration rate close to 2 mm day^{-1}. Accepting this value and using the average flux gradient of 0·86, over the period 18 January–7 March, between 0·05 and 0·3 m depth on plot 1 (data partly plotted on Fig. 4*a*), gives a value of $K = 2{\cdot}3$ mm day^{-1}. This is close to the geometric mean value of $K = 2{\cdot}0$ mm day^{-1} found for the measured values at this depth interval. Similarly, measured conductivity values from piezometers at greater depth agreed satisfactorily with those calculated from piezometric gradients and average flux.

The prediction of decreasing K with depth in a hydric profile (Philip 1968) could not be readily verified in this study, although the mean conductivity at 0·25 m depth (2–3 mm day^{-1}) was somewhat higher than that below 1 m (1–2 mm day^{-1}).

However, individual measurements showed considerable variation, and both the magnitude and spatial distribution of K appeared to be mainly determined by preferential flow paths.

The field average infiltration rate and derived hydraulic conductivity lie between the estimates from large and small rings, in contrast to the results of Ritchie *et al.* (1972), who found that K varied directly with size of sample area. They attributed this to the fact that preferential flow paths, such as slickensides, are not vertical and tend to be cut off along the sampler walls. We note in this regard that our depth/diameter ratio of about 0·2 for the rings was much less than 1, the average value used by Ritchie *et al.* (1972).

Swelling and Overburden Effects

The maximum vertical soil movement (Fig. 7) was 25 mm and involved swelling of soil material between 0·05 and 0·8 m depth (Fig. 6). This result is consistent with data collected by Aitchison and Holmes (1953) and Yaalon and Kalmar (1972), who reported maximum vertical movement at the soil surface of about 80 and 50 mm, respectively, for vertisols subjected to much larger differences in moisture content. Variation in surface elevation and changes in bulk density have obvious implications in calculating volumetric moisture content (Fig. 5) and in plotting relations such as shown in Fig. 6.

Values of α (Table 2) obtained near soil saturation were low, but *in situ* variability was high. However, differences in loaded ($\Psi + \Omega$) and unloaded (Ψ) potentials are quite noticeable. Such differences explain, at least partly, the frequently noted discrepancies between moisture characteristic curves obtained *in situ* for clay soils and those from vertically unconfined, but otherwise undisturbed, core samples (e.g. Talsma 1963).

References

Aitchison, G. D., and **Holmes, J. W.** (1953). Aspects of swelling in the soil profile. *Aust. J. Appl. Sci.* **4**, 244–59.

Allen, J. B., and **Braud, H. J.** (1966). Effects of cracks and initial moisture content on the infiltration rate of Sharkey clay. Bull. La. Agric. Exp. Stn. No. 163.

Allison, L. E. (1947). Effect of microorganisms on permeability of soil under prolonged submergence. *Soil Sci.* **63**, 439–50.

Avnimelech, Y., and **Nevo, Z.** (1964). Biological clogging of sands. *Soil Sci.* **98**, 222–6.

van Dijk, D. C., and **Talsma, T.** (1964). Soils of portion of the Coleambally irrigation area, N.S.W. CSIRO Aust. Soils and Land Use Ser. No. 47.

Philip, J. R. (1968). Moisture equilibrium in the vertical in swelling soils. I. Basic theory. *Aust. J. Soil Res.* **7**, 99–120.

Philip, J. R. (1969). Hydrostatics and hydrodynamics in swelling soils. *Water Resourc. Res.* **5**, 1070–7.

Philip, J. R. (1971). Hydrology of swelling soils. *In* 'Salinity and Water Use'. (Eds T. Talsma and and J. R. Philip.) pp. 95–107. (Macmillan: London.)

Ritchie, J. T., Kissel, D. E., and **Burnett, E.** (1972). Water movement in undisturbed swelling clay soil. *Proc. Soil Sci. Soc. Am.* **36**, 874–9.

Smiles, D. E. (1974). Infiltration into a swelling material. *Soil Sci.* **117**, 140–7.

Smiles, D. E., and **Colombera, P. M.** (1975). The early stages of infiltration into a swelling soil. *In* 'Heat and Mass Transfer in the Biosphere. I. Transfer Processes in the Plant Environment'. (Eds D. A. de Vries and N. H. Afgan.) pp. 77–85. (Scripta: Washington, D.C.)

Stirk, G. B. (1954). Some aspects of soil shrinkage and the effect of cracking upon water entry into the soil. *Aust. J. Agric. Res.* **5**, 279–90.

Swartz, G. L. (1966). Water entry into a black earth under flooding. *Qld. J. Agric. Anim. Sci.* **23**, 407–21.
Talsma, T. (1963). The control of saline groundwater. *Meded. Landbouwhogesch.* **63**(10), 1–68.
Talsma, T. (1969). *In situ* measurement of sorptivity. *Aust. J. Soil Res.* **7**, 269–76.
Talsma, T. (1976). Soil water movement: infiltration, redistribution, and ground water movement. Proc. 5th U.S./Aust. Range Sci. Seminar, Boise, Idaho, 1975. (Utah State Univ. Press: Logan.) (in press).
Talsma, T., and **van der Lelij, A.** (1976). Water balance estimates of evaporation from ponded rice fields in a semi-arid region. *Agric. Water Management* **1** (in press).
Yaalon, D. H., and **Kalmar, D.** (1972). Vertical movement in an undisturbed soil: continuous measurement of swelling and shrinkage with a sensitive appartus. *Geoderma* **8**, 231–40.

Manuscript received 24 May 1976